



Available online at [www.sciencedirect.com](http://www.sciencedirect.com)

ScienceDirect

journal homepage: [www.e-jmii.com](http://www.e-jmii.com)



Short Communication

# A *sbiT-sbiRS-gloI* regulatory circuit is involved in oxidative stress tolerance of *Stenotrophomonas maltophilia*

Cheng-Mu Wu<sup>a,1</sup>, Yi-Tzu Lee<sup>b,c,1</sup>, Hsu-Feng Lu<sup>d</sup>,  
Yen-Ling Lin<sup>a,e</sup>, Tsuey-Ching Yang<sup>a,\*</sup>



<sup>a</sup> Department of Biotechnology and Laboratory Science in Medicine, National Yang Ming Chiao Tung University, Taipei, Taiwan, ROC

<sup>b</sup> Department of Emergency Medicine, Taipei Veterans General Hospital, Taipei, Taiwan, ROC

<sup>c</sup> Faculty of Medicine, School of Medicine, National Yang Ming Chiao Tung University, Taipei, Taiwan, ROC

<sup>d</sup> Department of Medical Laboratory Science and Biotechnology, Asia University, Taichung, Taiwan, ROC

<sup>e</sup> Department of Medical Laboratory, Taipei Medical University-Shuang Ho Hospital, New Taipei City, Taiwan, ROC

Received 20 December 2023; received in revised form 1 June 2024; accepted 8 July 2024

Available online 14 July 2024

## KEYWORDS

*Stenotrophomonas maltophilia*;  
Glyoxalase I;  
Two-component regulatory system;  
Oxidative stress response

**Abstract** The *sbiT-sbiR-sbiS* operon of *Stenotrophomonas maltophilia* encodes an inner-membrane protein SbiT and a SbiS-SbiR two-component regulatory system. A *sbiT* mutant displayed a growth defect in LB agar. Mechanism studies revealed that *sbiT* deletion resulted in SbiSR activation and *gloI* upregulation, which increased intracellular ROS level and caused growth defect.

Copyright © 2024, Taiwan Society of Microbiology. Published by Elsevier Taiwan LLC. This is an open access article under the CC BY-NC-ND license (<http://creativecommons.org/licenses/by-nc-nd/4.0/>).

\* Corresponding author. Department of Biotechnology and Laboratory Science in Medicine, National Yang Ming Chiao Tung University, Taipei, Taiwan, ROC.

E-mail address: [tcyang@nycu.edu.tw](mailto:tcyang@nycu.edu.tw) (T.-C. Yang).

<sup>1</sup> Cheng-Mu Wu and Yi-Tzu Lee contributed equally to this work.

## Introduction

Oxidative stress is unavoidable in aerobic microorganisms. Reactive oxygen species (ROS) are produced through bacterial aerobic respiration and generated by the host immune system. To protect themselves against ROS-induced oxidative stress, bacteria have evolved different ROS defense mechanisms, including enzymatic ROS scavengers, non-enzymatic molecules, and efflux pumps.<sup>1</sup>

The glyoxalase system comprises a set of enzymes that detoxify reactive electrophilic species (RES). Glyoxal (GO) and methylglyoxal (MGO), the members of RES, can non-enzymatically modify nucleic acids and proteins, causing mutations. Glyoxalases include glutathione (GSH)-dependent enzymes, glyoxalase I (GloI) and glyoxalase II (GloII), and GSH-independent glyoxalase III (GloIII).<sup>2</sup> Although many bacterial *gloI* genes have been annotated in bacterial genomes, few bacterial GloI have been characterized.

Two-component regulatory systems (TCSs), composed of a sensor kinase (SK) and a response regulator (RR), are important mediators of signal transduction.<sup>3</sup> Genes encoding SK and RR are generally organized in an operon. However, it is sometimes observed that additional genes are in the same operon as the SK and RR genes. The proteins encoded by these additional genes may modulate the activity of SK or RR at the post-translational level.

*Stenotrophomonas maltophilia* is an emerging opportunistic pathogen in immunocompetent individuals. In our recent study, we disclosed a *sbiT-sbiR-sbiS* operon, a member of ferric uptake regulator (Fur) regulon, and elucidated its role in iron homeostasis.<sup>4</sup> The proteins encoded by *sbiR* and *sbiS* comprise a TCS, whose activation is transcriptionally regulated by Fur and post-translationally modulated by SbiT via SbiT–SbiS interaction. Activated SbiR upregulates the expression of SmeDEF and SbiAB pumps, which contribute to stenobactin secretion.<sup>4</sup> In that study, we noticed that a *sbiT* mutant, K $\Delta$ SbiT, displayed a compromised growth in LB agar.<sup>4</sup> In this study, we attempted to elucidate the underlying mechanism for the  $\Delta$ *sbiT* phenotype.

## Materials and methods

### Transcriptome analysis

Total RNA isolation, DNase treatment, rRNA depletion, adapter-ligated cDNA library construction and enrichment, and cDNA sequencing, were performed as described previously.<sup>4</sup> The output R1 reads were mapped to the genome of K279a. Gene enrichment analysis was conducted using topGo v2.44.0 with Fisher's exact test and Weight 01 algorithm. The total number of reads per gene was normalized by transcripts per kilobase million (TPM) values.

### Construction of deletion mutant K $\Delta$ GloI

Two DNA fragments flanking N-terminus and C-terminus of *gloI* gene were amplified via PCR using the primer sets of GloIN-F/R and GloIC-F/R (Suppl. Table 1), respectively, and subsequently cloned into pEX18Tc, generating p $\Delta$ GloI (Suppl. Table 1). Transconjugant selection and double

crossover mutant confirmation were performed as described previously.<sup>4</sup>

### Intracellular iron level determination

The logarithmical phase cells were collected and resuspended in 2 mL of Milli-Q water. The cell suspension was sonicated, centrifuged, and filtered through a 0.45-mm-pore-size Millipore. Bacterial aliquot was collected for inductively coupled plasma-mass spectrometry (ICP-MS) assay (Agilent 7700e instrument, Agilent Technologies, USA). Cell numbers in bacterial aliquot were determined by CFU counting. Iron level was normalized by the cell numbers. The commercially available iron standards were included as a control.

### Intracellular ROS level determination (DCFH-DA assay)

The logarithmical-phase bacterial culture was treated with DCFH-DA (final concentration 0.01  $\mu$ M) for 1 h at 37 °C. A cell-free LB broth with DCFH-DA was used as a blank control. To monitor DCFH-DA oxidation, the fluorescence intensity was measured at 488 nm excitation and 520 nm emission. The bacterial mass was determined by recording the optical density at 450 nm (OD<sub>450nm</sub>). Intracellular ROS level was expressed as fluorescence intensity/OD<sub>450nm</sub>.

### Glyoxalase I activity assay

The glyoxalase I activity was determined using Glyoxalase I activity Assay Kit (Sigma–Aldrich, Missouri, USA) and activity was calculated according to the formula provided by the manufacturer. The specific activity of glyoxalase I was expressed as glyoxalase I activity/mg protein. Protein concentration was determined using the Bio-Rad protein assay reagent, with bovine serum albumin as a standard.

## Results

### Inactivation of *sbiT* results in a growth defect in a *sbiRS*-dependent manner

K $\Delta$ SbiT exhibited a growth defect in LB agar (Suppl. Fig. 1A), and this phenotype was confirmed by monitoring bacterial growth in LB broth (Suppl. Fig. 1B). Furthermore, we noticed that growth defect observed in K $\Delta$ SbiT was restored to the wild-type level when  $\Delta$ *sbiRS* was introduced into the K $\Delta$ SbiT (Suppl. Fig. 1). Thus, inactivation of *sbiT* results in a growth defect in a *sbiSR*-dependent manner.

### K $\Delta$ SbiT experiences a ROS stress, not an iron-overload stress

For the  $\Delta$ *sbiT*-mediated growth defect, we assumed that *sbiT* deletion leads to SbiSR TCS activation, which makes K $\Delta$ SbiT experience an iron-overload stress. To test this hypothesis, 2,2'-dipyridyl (DIP) tolerance and intracellular iron levels were investigated. KJ and K $\Delta$ SbiT displayed comparable viability in the DIP-containing plates (Fig. 1A) and comparable intracellular iron levels (Fig. 1B).

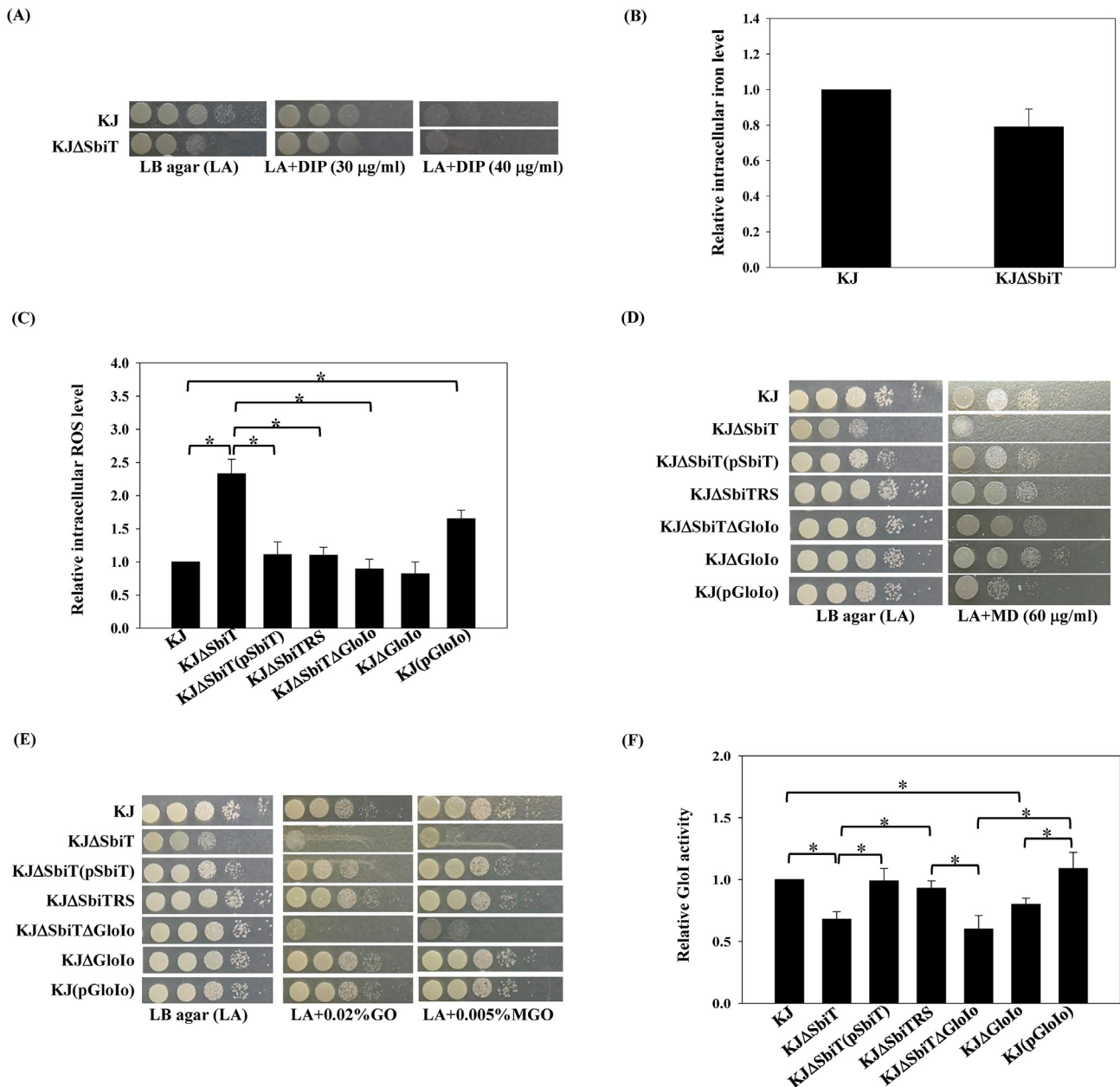


**Figure 1. Role of *sbiTRS* operon and *gloIo* in iron-depleted, ROS, and RES stress.**

(A) The impact of *sbiT* inactivation on DIP tolerance. Logarithmic phase bacterial cells of  $2 \times 10^5$  cfu/ $\mu$ l were serially 10-fold diluted. Bacterial suspensions (5  $\mu$ l) were spotted onto LB agar with and without DIP. After 24-h incubation at 37 °C, the growth of bacterial cells was observed. DIP, 2, 2-dipyridyl. (B) The intracellular iron levels of wild-type KJ and KJ $\Delta$ SbiT. The amount of iron in the logarithmically grown wild-type KJ and KJ $\Delta$ SbiT was determined by inductively coupled plasma mass spectrometry (ICP-MS). The relative iron level was calculated using the iron level of KJ cells as 1. Bars represent the average values from three independent experiments. Error bars represent the standard errors of means. (C) The intracellular ROS levels of KJ and its derived constructs. The bacterial cells tested were cultured in LB medium containing DCFH-DA for 5 h and the fluorescence at 550 nm was determined. The relative fluorescence is normalized to the fluorescence of wild-type KJ. \* $P < 0.01$ , significance calculated by Student's *t* test. (D) The MD susceptibility of KJ and its derived constructs. Logarithmic phase bacterial cells of  $2 \times 10^5$  cfu/ $\mu$ l were serially 10-fold diluted. Bacterial suspensions (5  $\mu$ l) were spotted onto LB agar with and without MD. After 24-h incubation at 37 °C, the growth of bacterial cells was observed. MD, menadione. (E) Cell viabilities of wild-type KJ and its derived constructs in GO- and MGO-containing medium. Logarithmic phase bacterial cells of  $2 \times 10^5$  cfu/ $\mu$ l were serially 10-fold diluted. Bacterial suspensions (5  $\mu$ l) were spotted onto LB agar with and without GO (or MGO). After 24-h incubation at 37 °C, the growth of bacterial cells was observed. (F) The intracellular glyoxalase I activities of wild-type KJ and its derived constructs. The bacterial cells tested were cultured in LB medium containing DCFH-DA for 5 h and the fluorescence at 550 nm was determined. The relative GloI activity was calculated using the GloI activity of wild-type KJ cells as 1. Bars represent the average values from three independent experiments. Error bars represent the standard errors of means. \* $P < 0.01$ , significance calculated by Student's *t* test.

Given that ROS levels and iron toxicity are closely associated *in vivo*, we wondered whether growth defect of KJΔ*SbiT* is related to intracellular ROS levels. Relative to that in wild-type KJ, the ROS level in KJΔ*SbiT* had a  $2.33 \pm 0.22$ -fold increment and reversed to wild-type level in KJΔ*SbiT*(p*SbiT*) and KJΔ*SbiTRS* (Fig. 1C). Furthermore, KJΔ*SbiT* was more susceptible to menadione (MD) than wild-type KJ, but KJΔ*SbiT*(p*SbiT*), KJΔ*SbiTRS*, and KJ had comparable susceptibility to MD (Fig. 1D). Collectively, KJΔ*SbiT* experiences a ROS stress, not an iron-overload stress.

### GloI upregulation in KJΔ*SbiT* contributes to increased ROS level and MD susceptibility

Based on the above results, we speculated that some gene(s) of the *SbiSR* regulon are involved in the Δ*SbiT*-mediated decrease in MD tolerance. RNAseq transcriptome analysis of KJ, KJΔ*SbiT*, and KJΔ*SbiTRS* was conducted to reveal the *SbiSR* regulon. The gene expression changes greater than threefold was defined as significant. We aimed to search for candidate gene(s) whose expression was significantly upregulated (or downregulated) in KJΔ*SbiT* and tended to revert to wild-type KJ levels in KJΔ*SbiTRS*. In total, 68 genes matched this criterion (Suppl. Table 2). Among the 68 candidate genes (Suppl. Table 2), *smlt0186* transcript showed the greatest change in KJΔ*SbiT*. *smlt0186* expressions in KJ, KJΔ*SbiT*, and KJΔ*SbiTRS* were validated by qRT-PCR (Suppl. Fig. 2). *smlt0186* is annotated as a glyoxalase gene in *S. maltophilia* K279a. Genome-wide survey on K279a revealed 12 annotated glyoxalase genes (Suppl. Table 3). Phylogenetic analysis of the 12 GlOs and the characterized GlOs from other bacteria was conducted (Suppl. Fig. 3). Based on the phylogenetic analysis and the following findings, we designated *Smlt0186* as GloI (O indicates oxidative stress).

To clarify contribution of *gloI* upregulation to Δ*SbiT*-mediated decrease in MD tolerance, a *sbiT* and *gloI* double deletion mutant, KJΔ*SbiT*Δ*GloI*, was constructed. Compared to KJΔ*SbiT*, KJΔ*SbiT*Δ*GloI* reverted ROS level and MD susceptibility to wild-type level (Fig. 1C & D), indicating that *GloI* upregulation contributes to Δ*SbiT*-mediated increase in ROS level MD susceptibility. The impact of *gloI* deletion or overexpression on the ROS level and MD susceptibility of wild-type KJ were also assessed. Compared with wild-type KJ, KJΔ*GloI* displayed comparable ROS level and MD susceptibility; however, KJ(p*GloI*) had increased ROS level and MD susceptibility (Fig. 1C & D), further supporting the positive contribution of *GloI* upregulation to ROS level and MD susceptibility.

### GloI upregulation is irrelevant to Δ*SbiT*-mediated decrease of GO/MGO tolerance and Glol activity.

Given that glyoxalase contributes to RES detoxification,<sup>2</sup> we investigated GO/MGO tolerance and Glol activities of wild-type KJ and its derived constructs. Compared to wild-type KJ, KJΔ*SbiT* displayed decreased GO/MGO tolerance (Fig. 1E) and Glol activity (Fig. 1F) and these compromises were reverted to wild-type levels when *sbiT* was complemented or *sbiRS* was further deleted (Fig. 1E & F).

However, *gloI* deletion from KJΔ*SbiT* did not further decrease GO/MGO tolerance (Fig. 1E) and Glol activity (Fig. 1F), indicating that *gloI* upregulation is irrelevant to Δ*SbiT*-mediated decrease of GO/MGO tolerance and Glol activity. We wonder whether *GloI* harbors Glol activity; thus, KJΔ*GloI*, a *gloI* deletion mutant, and KJ(p*GloI*), a *gloI* overexpression strain, were subjected to Glol activity assay. KJΔ*GloI* displayed lower Glol activity than wild-type KJ and KJ(p*GloI*) (Fig. 1F), supporting the presence of Glol activity in *GloI*.

## Discussion

Glyoxalase I (Glol) is a member of the glyoxalase system and known to be involved in RES detoxification.<sup>2</sup> In this study, we revealed that the *GloI* protein of *S. maltophilia* has a significant impact on ROS stress and is less related to RES stress. A bacterial Glol displaying additional functions beyond RES detoxification has been reported in *E. coli*. The Glol of *E. coli* functions in potassium homeostasis because Glol activity is proportional to the activation level of the KefB and KefC potassium efflux pumps.<sup>5</sup> In this study, we firstly report that *gloI* overexpression resulted in increased intracellular ROS levels (Fig. 1C) and MD susceptibility (Fig. 1D), but hardly impacted on GO/MGO tolerance (Fig. 1E). Therefore, *GloI* may represent an unrecognized class of glyoxalase I enzymes, harboring some unidentified enzyme activities, in addition to glyoxalase activity. We speculated that *GloI* activity may contribute to the increase in ROS levels and/or decrease in ROS alleviation.

*sbiTRS* operon, a member of *Fur* regulon, is moderately expressed in logarithmically grown wild-type KJ, but *SbiSR* TCS keeps in a resting condition due to *SbiT*–*SbiS* interaction.<sup>4</sup> In an iron-depleted condition, *Fur* loses its binding affinity to *Fur* box and the *SbiT*–*SbiS* interaction disappears, resulting in the high-level activation of *SbiSR* TCS, which provides a benefit to bacteria for iron source acquisition.<sup>4</sup> In this study, we further demonstrated that KJΔ*SbiT* displayed a growth defect in LB agar, but not in DIP-containing LB agar (Fig. 1A), indicates that activation of *SbiSR* TCS in an iron replete condition is detrimental to bacteria, making them more sensitive to ROS. Thus, the two-brake implement of *Fur* and *SbiT* prevents bacteria from *SbiSR* over-activation in an iron replete condition.

Increased intracellular ROS level seems to be a short-coming for bacteria; however, the impact of ROS on the development of antibiotic resistance cannot be ignored. Several antibiotic resistance mechanisms are triggered by ROS<sup>6,7</sup> and some oxidative stress alleviation systems can cross-protect bacteria from antibiotic challenges.<sup>8–10</sup> Therefore, a bacterium with an elevated intracellular ROS level, such as KJΔ*SbiT* in this study, is prone to resistance development.

## Funding

This work was supported by National Science and Technology Council of Taiwan (grant no. MOST 111-2320-B-A49-025-MY3 & NSTC 112-2320-B-A49-043-MY3) and the Professor Tsuei-Chu Mong Merit Scholarship (grant number 410260001).

## CRedit authorship contribution statement

**Cheng-Mu Wu:** Formal analysis, Methodology, Writing – original draft, Writing – review & editing. **Yi-Tzu Lee:** Conceptualization, Data curation, Resources, Writing – original draft, Writing – review & editing. **Hsu-Feng Lu:** Conceptualization, Data curation, Writing – review & editing. **Yen-Ling Lin:** Data curation, Methodology, Writing – review & editing. **Tsuey-Ching Yang:** Conceptualization, Funding acquisition, Investigation, Project administration, Supervision, Writing – review & editing.

## Declaration of competing interest

The authors declare that the research was conducted in the absence of any commercial or financial relationships that could be construed as a potential conflict of interest.

## References

1. Imlay JA. Cellular defenses against superoxide and hydrogen peroxide. *Annu Rev Biochem* 2008;**77**:755–76.
2. Thornalley PJ. The glyoxalase system: new developments towards functional characterization of a metabolic pathway fundamental to biological life. *Biochem J* 1990;**269**:1–11.
3. Gao R, Stock AM. Biological insights from structures of two-component proteins. *Annu Rev Microbiol* 2009;**63**:133–54.
4. Wu CM, Li LH, Lin YL, Wu CJ, Lin YT, Yang TC. The *sbiTRS* operon contributes to stenobactin-mediated iron utilization in *Stenotrophomonas maltophilia*. *Microbiol Spectr* 2022;**10**:e0267322.
5. MacLean MJ, Ness LS, Ferguson GP, Booth IR. The role of glyoxalase I in the detoxification of methylglyoxal and in the activation of KefB K<sup>+</sup> efflux system in *Escherichia coli*. *Mol Microbiol* 1998;**27**:563–71.
6. Wu CJ, Chiu TT, Lin YT, Huang YW, Li LH, Yang TC. Role of *smeU1VWU2X* operon in alleviation of oxidative stresses and occurrence of sulfamethoxazole-trimethoprim resistant mutants in *Stenotrophomonas maltophilia*. *Antimicrob Agents Chemother* 2018;**62**:e02114-17.
7. Li LH, Wu CM, Lin YT, Pan SY, Yang TC. Roles of FadRACB system in formaldehyde detoxification, oxidative stress alleviation and antibiotic susceptibility in *Stenotrophomonas maltophilia*. *J Antimicrob Chemother* 2020;**75**:2101–9.
8. Lin YT, Huang YW, Liou RS, Chang YC, Yang TC. MacABCsm, an ABC-type tripartite efflux pump of *Stenotrophomonas maltophilia* involved in drug resistance, oxidative and envelope stress tolerance and biofilm formation. *J Antimicrob Chemother* 2014;**69**:3221–6.
9. Li LH, Lu HF, Liu YF, Lin YT, Yang TC. *FadACB* and *smeU1VWU2X* contribute to oxidative stress-mediated fluoroquinolone resistance in *Stenotrophomonas maltophilia*. *Antimicrob Agents Chemother* 2022;**66**:e0204321.
10. Liao CH, Ku RH, Li LH, Wu CM, Yang TC. Role of *yceA-cybB-yceB* operon in oxidative stress tolerance, swimming motility and antibiotic susceptibility of *Stenotrophomonas maltophilia*. *J Antimicrob Chemother* 2023;**78**:1891–9.

## Appendix A. Supplementary data

Supplementary data to this article can be found online at <https://doi.org/10.1016/j.jmii.2024.07.005>.